Synthesis of Calcium Silicate Hydrate Nanocomposites and Its Influence on the Hydration Process of Cement

Jinlong Zhang*[a,b], Conghao Zhong[a], Jiabing Hu[a], Qiang Shao[a], Kaihong Zhong*[a]

[a] Guangzhou Institute of Building Science Group Co., Ltd., Guangzhou, Guangdong 510440, People's Republic of China.
[b] Guangzhou Municipal Construction Group Co., Ltd., Guangzhou, Guangdong 510030, People's Republic of China.
zhangjl117@126.com

Abstract. It is essential to investigate the influence of calcium-silicate-hydrate (C-S-H) nanocomposites on the hydration process of cement at different dosages. This study presents the synthesis of C-S-H nanocomposites (NC) via coprecipitation and characterization using DLS, TEM, XRD, and FT-IR. The influence of varying quantities of NC on the hydration process of cement was examined, including setting time, compressive strength, hydration heat release, and microstructural morphology of hydration products. Furthermore, correlations between hydration microstructure evolution and macroscopic performance were identified. The results indicate that NC significantly reduce the setting time of cement paste; however, the effect on initial setting time diminishes with increasing dosage. Compared to the blank system, NC notably enhance the compressive strength of cement mortar at 1 day of curing. But, after 3 days, the positive effect of NC on strength development diminishes, and at a 1% dosage, there is virtually no improvement in compressive strength. Thermal hydration tests and SEM analysis demonstrate that NC primarily accelerate cement hydration and enhance compressive strength development by promoting the formation of a cross-linked hydration product network. Nonetheless, the rapid growth of hydration products can increase the number of inter gel pores, thereby reducing the strengthening effect at higher dosages over 3 days of curing.

Keywords: C-S-H nanocomposites; dosage variation, hydration acceleration; microstructure evolution

1 Introduction

With the development of industrialization in construction has led to the prefabrication of concrete components becoming essential for achieving high-quality and sustainable development in the construction industry. During the production of prefabricated components, steam curing is generally employed to accelerate the early strength development of concrete, thereby enhancing production efficiency. However, the application of steam curing can result in thermal damage to components, which

W. Guo et al. (eds.), *Proceedings of the 3rd International Conference on Green Building, Civil Engineering and Smart City (GBCESC 2024)*, Advances in Engineering Research 264,
https://doi.org/10.2991/978-94-6463-728-1_62

may negatively impact their long-term durability. Additionally, for components with unconventional dimensions, curing becomes impractical, and the energy-intensive curing process significantly increases carbon emissions during production.

In recent years, numerous researchers have demonstrated that the incorporation of nanomaterials into cementitious materials can markedly accelerate the cement hydration process and enhance the early mechanical properties of concrete [1-3]. Among these materials, NC, as the main hydration product of cement [4], exhibit superior early strength effects compared to other nanomaterials. NC effectively promote the cement hydration process, thereby enhancing the early strength of concrete [5,6]. To achieve well-dispersed NC with stable properties and mitigate negative effects from particle aggregation, PCE is typically used as a dispersant, and NC is synthesized via coprecipitation methods [7-9].

Despite extensive research analyzing the early strength mechanisms and influencing factors of NC, limited investigation has been conducted into the dissolution-precipitation theory based on cement hydration to elucidate its mechanisms at different hydration stages. Therefore, this study employs coprecipitation methods to optimize synthesis parameters and prepare stable, non-precipitating NC while characterizing their performance parameters. Techniques such as hydration calorimetry and SEM analysis are utilized to explore the effects of different amounts of nano-C-S-H on different stages of cement hydration, with the aim of elucidating the early strength mechanisms of NC.

2 Experimental section

2.1 Raw materials

The experiment utilized P·I 42.5 Portland cement produced by the Qufu Zhonglian Cement Company, which complies with the GB 8076—2008 standards for admixture testing. The reagents used in the experiment included calcium nitrate tetrahydrate, sodium metasilicate nonahydrate, sodium hydroxide, and nitric acid, all of which were purchased from Shanghai Aladdin Bio-Chem Technology Co., Ltd. The PCE (40% solid content, pH=5.86), obtained from Guangzhou Academy of Building Research Group Co., Ltd.

2.2 Synthesize of NC

This study employed a coprecipitation method to synthesize NC[10]. The following solutions were prepared: a 215 g solution of calcium nitrate with a mass fraction of 33.75%, a 310 g solution of sodium silicate with a mass fraction of 16.02%, and a 30 wt% sodium hydroxide solution. In four-necked flasks, 98 g of polycarboxylate ether dispersant and 316 g of deionized water were measured, and sodium hydroxide was added to adjust the solution to pH 11. After that the calcium nitrate were added continuously at 1.20g/min and the sodium silicate were added continuously at 1.72g/min to the PCE solution while stirring at 600 r/min, the pH was maintained at 11, and the reaction temperature was kept at 25°C. After the addition

was complete, the mixture was continuously stirred for 24 hours to obtain a suspension of NC.

2.3 Testing

Microscopic characterizations

The samples underwent phase analysis using a Rigaku Miniflex 600 X-ray diffractometer (Japan), with a scanning range of 5° to 90°, a step size of 0.02° (2θ), and a scanning time of approximately 17 min. For FT-IR spectroscopy, a Nicolet iS10 FT-IR instrument (USA) was employed to analyze the absorption spectra of both the PCE dispersant and the synthesized nano-C-S-H, with a constant spectral resolution of R=4 cm^{-1} over the wavenumber range of 400-4000 cm^{-1}. The morphological characterization of the C-S-H nanocomposite particles was conducted using a JEM-2100 TEM from JEOL Ltd. (Japan). Prior to measurement, the NC were diluted 100-fold, applied to a carbon support film with a mesh size of 200, dried under vacuum at 40°C, and then observed. The particle size distribution in the C-S-H nanocomposite suspension was determined using a Mastersizer 2000 dynamic light scattering instrument. The samples were diluted with deionized water to a concentration of approximately 0.1 before the measurement was made.

Setting time

In accordance with the standards set forth in GB/T1346-2011, a Vicat apparatus was employed to determine the impact of NC on the initial and final setting times of cement pastes. The specific mix proportions are outlined in Table 1. Prior to each test, meticulous care was taken to clean the probe to remove any residual cement paste, ensuring that it would not affect subsequent tests.

Table 1. Mix proportion of the Setting time test samples/(g)

Sample	Cement	water	NC
Blank	450	180	0
C-S-H0.2%	450	176.4	4.5
C-S-H0.6%	450	169.2	13.5
C-S-H1.0%	450	162	22.5

Compressive strengths.

The compressive strength test was conducted on mortar specimens prepared with a mass ratio of 1 (base cement) : 3 (standard sand) : 0.4 (water). The specimens, measuring 40 × 40 × 160 mm, incorporated nano C-S-H in quantities consistent with those used in the setting time tests. These specimens were cured under standard conditions, and their compressive strength was evaluated after 1 d, 3 d, 7 d, and 28 d of curing.

Hydration heat release.

The impact of NC on the hydration heat of cement was quantified using an eight-channel isothermal calorimeter (TAM Air). The specific mix proportions are

delineated in Table 1. For each test, 10 g of cement paste was used, with the test temperature maintained at 20°C for 72 h.

Scanning electron microscopy.

The microscopic morphology of cement samples at various ages with added NC was observed using the German ZEISS Sigma 300 ultra-high resolution scanning electron microscope.

3 Results and discussion

3.1 Characterization of NC

Fig. 1(a) illustrates that the C-S-H nanocomposite suspension show a single peak distribution, indicating a stable particle size range from 90 to 460 nm with a median particle size of 162 nm. The TEM image (Fig. 1(b)) reveals that C-S-H nanocomposite particles exhibit a wrinkled film-like gel structure, with particle lengths of approximately 200 nm.

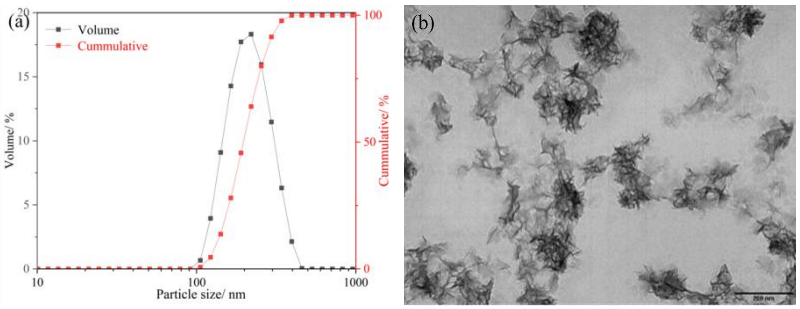

Fig. 1. Characterization of NC: (a) particle size distribution, (b) TEM image of NC.

The XRD pattern of the NC is also investigated, as shown in Fig. 2(a). The characteristic peaks of C-S-H are observed at 2θ = 19.1°, 29.4°, 49.9°, and 55°, corresponding to the d_{100}, d_{110}, d_{020}, and d_{112} basal reflections of the C-S-H structure, respectively. The broad diffraction peaks indicate a low degree of crystallinity in the NC. The peaks at 2θ = 29° and 39° are attributed to calcite ($CaCO_3$) reflections, suggesting the presence of a small amount of $CaCO_3$ due to carbonation during synthesis. Additionally, the (d_{002}) reflection of C-S-H at 2θ = 7° represents the spacing between the silicate chains in the C-S-H structure [11,12]. Compared to inorganic C-S-H, the NC prepared with PCE as a dispersant exhibit a distinct diffraction peak at 2θ = 7°, suggesting that PCE molecules intercalate between the layers of C-S-H, reducing its crystallinity and leading to the disappearance of the basal d_{002} reflection. Fig. 2(b) illustrates the infrared spectrum of NC and PCE. The characteristic stretching vibrations of the silicate units are observed at 966 cm^{-1}, 650 cm^{-1}, and 441 cm^{-1}, corresponding to the Q^2 Si-O stretching vibrations, υ(Si-O-Si), and δ(Si-O-Si) within the C-S-H structure [13]. In addition to the characteristic peaks

of inorganic C-S-H, the stretching vibrations of $-CH_2-CH_3$ and C-O at 2918 cm^{-1} and 1349 cm^{-1}, respectively, confirm the presence of PCE molecules in the synthesized NC [14].

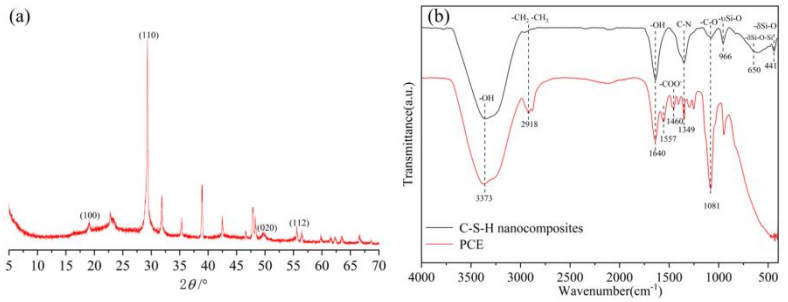

Fig. 2. XRD spectra and FT-IR spectra of NC: (a) XRD, (b) FT-IR.

3.2 Setting times

The impact of NC on the setting times of cement under varying dosage is illustrated in Fig. 3(a). The NC have a notable impact on both the initial and final setting times of the cement paste. The initial setting time of the blank cement paste is 295 min, while the final setting time is 510 min. With the addition of NC at a dosage of 0.2%, the initial setting time decreases to 218 min, and the final setting time decreases to 345 min.

However, as the dosage of NC increases, the effect on shortening the initial setting time gradually diminishes. As shown in Fig. 3(b), with the dosage increasing from 0.6% to 1.0%, a reduction of only 12 min in the initial setting time and 27 min in the final setting time is observed. This results show that the effect of NC on the setting times of cement is not linear.

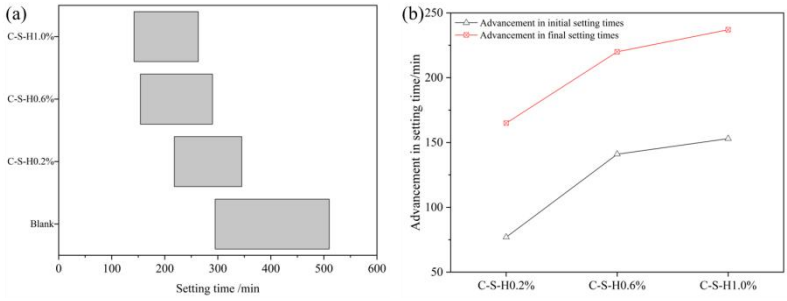

Fig. 3. The setting times of cement paste with NC,(a) interval between initial and final setting times, (b) the advancement in setting times relative to the control group.

3.3 Strength development of mortar

The Fig. 4(a) shows that NC enhance the early-age compressive strength of cement mortar. Compared to the 24 h compressive strength of the control group, the incorporation of 0.2% NC results in an increase from 19.94 MPa to 25.89 MPa,

representing a 29.83% enhancement. The strength further increases with elevated dosages, reaching 28.41 MPa at a 1% dosage. However, as the curing age increases, the enhancement of mortar strength by NC diminishes. As illustrated in Figure 4(b), the enhancement effect of NC at a 1% dosage on mortar strength significantly diminishes after 3 days of curing, showing notably lower strength than that observed at 0.2% and 0.6% dosages. At the 28 day curing period, the strength of the mortar with 1% nano C-S-H is almost identical to that of the control group. Those results demonstrate that NC effectively enhances the early-age strength of cement mortar.

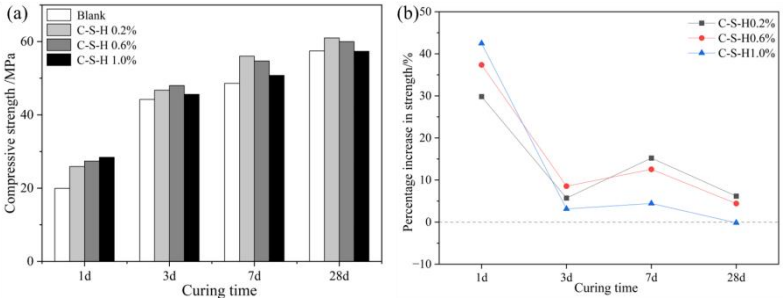

Fig. 4. (a) Compressive strength development of mortar prepared with 0.2wt%,0.6wt% and1.0wt % NC, (b) percentage increase in compressive strength with different dosages of NC.

3.4 Hydration heat evolution

In order to gain insight into the impact of varying NC dosages on the mechanism of action, the hydration heat release rate of cement paste was monitored. As shown in the Fig. 5(a), NC significantly reduce the duration of the induction period and enhance the hydration heat release rate during this phase. This promoting effect increases with higher dosages, rising from an initial 0.655 mW/g to 0.91 mW/g. Simultaneously, the hydration heat peak and its appearance time are advanced. Specifically, the hydration heat peak and its appearance time shift from 12.32 h in the control system to 7.93 h and 6.72 h, respectively. Notably, NC cause a continuous increase in the hydration heat shoulder peak, which subsequently merges into the main heat release peak. When the dosage of NC exceeds 0.2%, the hydration heat shoulder peak essentially disappears and merges completely into the main peak. The hydration heat shoulder peak is primarily attributed to the secondary hydration of tricalcium aluminate (C_3A) in cement clinker [15]. This indicates that NC accelerate the consumption of SO_4^{2-} in the cement system, thereby promoting the early hydration of C_3A.

The Fig. 5(b) shows that NC increase the total hydration heat release, with cumulative heat release continuing to rise with higher dosages. At a dosage of 0.2%, the cumulative heat release at 72 h increases from 286.73 J/g to 298.97 J/g. With an increase in dosage to 1%, the cumulative heat release rises to 323.04 J/g. It is notable that as the dosage of NC increases, the promoting effect on cumulative hydration heat release diminishes.

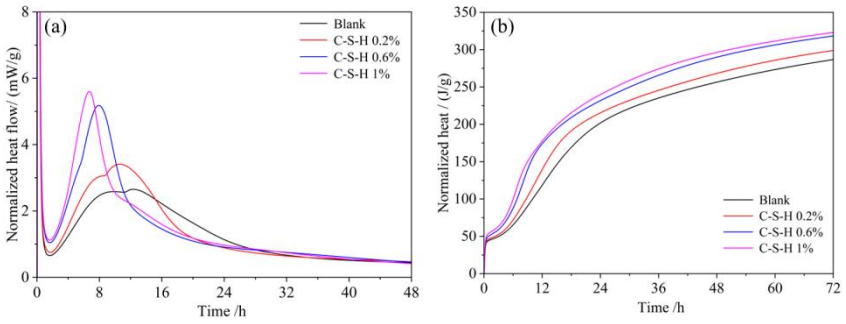

Fig. 5. The effect of NC on cement hydration: (a) Heat flow; (b) Cumulative heat release

3.5 SEM images of hydration products

In order to analyze the effect of different amounts of NC on the cement hydration process, two key points were selected to observe the microstructural features of hydration products in both blank cement and cement systems containing 1% NC at different stages of hydration. Based on the hydration heat release curve, the selected points were the induction period and the peak hydration heat release.

As shown in Fig. 6(a), during the induction period, isolated hexagonal prism-shaped ettringite crystals and needle-like C-S-H gel are sparsely distributed on the surface of cement particles. The addition of 1% NC results in a notable increase in the quantity of hydration products observed on the surface of cement particles, accompanied by the presence of etch pits. This suggests that NC accelerate the dissolution of cement particles. The increased concentration of ions in the cement pore solution leads to a notable increase in the number of hydration products on the surface of unhydrated cement particles. Fig. 6(b) illustrates the microstructural morphology at the peak of the hydration heat release in the blank system, showing a significant increase in hydration products that completely cover the surface of cement particles, primarily consisting of needle-like C-S-H gel. In contrast, Fig. 6(d), depicting the system with added NC, displays denser C-S-H gel structures that interconnect between particles. This indicates that NC effectively promote the precipitation and growth of hydration products.

The findings of this study reveal that NC effectively reduces the nucleation energy barrier for hydration products by providing advantageous nucleation surfaces. This facilitates the rapid formation of a reliable cross-linked network within the cement paste, significantly shortening the setting time and rapidly increasing early compressive strength. Notably, a system containing 1% NC exhibited a decrease in compressive strength after 3 d of curing. These results suggest an optimal dosage of NC that maximizes the macroscopic performance of cement-based materials, and this optimal dosage does not align with the thermodynamic impact of NC on cement hydration. The microscopic morphology of hydration products, as shown in Figure 6, indicates that the incorporation of 1% NC significantly increases the quantity of hydration products at the same hydration stage. Additionally, with increasing curing age, the needle length and density of the generated C-S-H are significantly higher

than those in the control group and the system with 0.6% NC. The accelerated growth of these hydration products results in shorter setting times and higher hydration heat release. However, the rapid growth of C-S-H gel increases the gel interstitial pores, leading to a decrease in matrix strength. At earlier curing ages, the generation of hydration products predominates, which is consistent with the compressive strength development pattern discussed in Section 2.3.3.

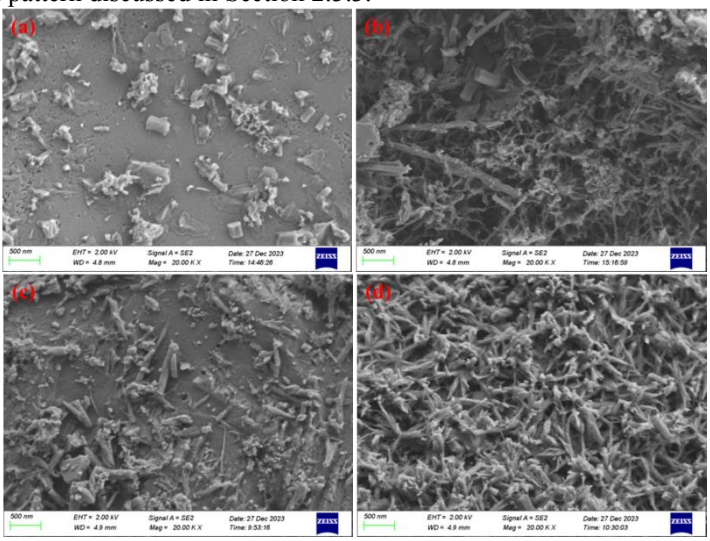

Fig. 6. Morphology of cement hydration products with 1.0% addition of NC: (a) Blank-1.67 h, (b) Blank-12.32 h, (c) 1%NC-1.62 h, (d) 1%NC-6.72 h.

4 Conclusions

The following conclusions can be drawn from this study:

(1) The NC with a single peak distribution and folded sheet-like condensation structure were synthesized by coprecipitation. Setting time and Strength development of mortar test illustrates that the NC should effectively shorten the setting time and increase the early strength of mortar.

(2) At the 1 d age, increasing the dosage of NC results in a more pronounced enhancement of strength, with a 1% dosage leading to an approximately 49.5% increase in strength. However, beyond the 3-day age, excessive dosages diminish the strength enhancement effect.

(3) Calorimetry results showed that NC can effectively shorten the induction period and increase the cumulative heat release of cement hydration, with the effect becoming more pronounced as the dosage increases. However, at higher dosages, the enhancement effect on cumulative heat release diminishes.

(4) SEM tests demonstrate that NC significantly increase the generation of hydration products during the induction period, enhancing the density of hydration products during the acceleration period and increasing the length of C-S-H gel.

Acknowledgment

This work was financially supported by the National Natural Science Foundation of China（52341801、52378332）, the Science and Technology Innovation Plan Project of Guangdong Provincial Department of Housing and Urban Rural Development (2022-K25-212467), the science and technology planning project of Guangzhou Municipal Construction Group Co., Ltd. and Guangzhou Institute of Building Science Group Co., Ltd. (Nos. [2021]-KJ015, [2023]-KJ020 and 2023 Y-KJ03).

References

1. Wang K, Liu F, Yang F, et al. Study on the effect of C-S-H nanocrystalline nuclei on the hydration properties of mineral admixture composite cementitious materials [J]. Bulletin of the Chinese Ceramic Society,2022,41(07).
2. Chen H, Tang M X. Opportunities and challenges for application of nano-material in civil engineering[J]. GUANGZHOU ARCHITECTURE, 2017, 45(02): 2-8.
3. Chen W, Gu B Q, Study on the correlation between random variables and ultimate bearing capacity of steel tubular scaffold with couplers[J]. GUANGZHOU ARCHITECTURE, 2022, 50(05): 52.
4. Zheng X, Yu P, Xie Y, et al. C-S-H Early Strength Agent Research Status Review [J]. Concrete ,2021, (10):119-123.
5. Theobald M, Plank J. C-S-H-Polycondensate nanocomposites as effective seeding materials for Portland composite cements[J]. Cement and Concrete Composites, 2022, 125: 104278.
6. Li J, Zhang W, Xu K, et al. Fibrillar calcium silicate hydrate seeds from hydrated tricalcium silicate lower cement demand[J]. Cement and Concrete Research, 2020, 137: 106195.
7. Lei F, Lei L, Kang Y, et al. Effect of 2-acrylamide-2-methylpropane sulfonic acid on the early strength enhancement of calcium silicate hydrate seed[J]. Cement and Concrete Composites, 2024, 149: 105527.
8. Wang F, Kong X, Wang D, et al. The effects of nano‐C‐S‐H with different polymer stabilizers on early cement hydration[J]. Journal of the American Ceramic Society, 2019, 102(9): 5103-5116.
9. Zhang J L, Wang Z M, Yao Y H, et al. The effect and mechanism of C-S-H-PCE nanocomposites on the early strength of mortar under different water-to-cement ratio[J]. Journal of Building Engineering, 2024, 44, 103360.
10. Shao Q Shi L, Tang X P, et al. The effect of acid-ether ratio on the performance of C-S-H/PCE/DL-AL crystal nucleus early strength agent[J]. GUANGZHOU ARCHITECTURE, 2023, 51(06): 79.
11. Pang J L, Wang J Y, Xu M Q, et al. C-S-H/PCE gel on the low temperature and early strength properties of phosphate slag cement [J]. Cement ,2022, (01):17-20.
12. Plank J, Li H, Ilg M, et al. A microstructural analysis of isoprenol ether-based polycarboxylates and the impact of structural motifs on the dispersing effectiveness[J]. Cement and Concrete Research, 2016, 84: 20-29.

13. Rashad A M. A synopsis about the effect of nano-Al_2O_3, nano-Fe_2O_3, nano-Fe_3O_4 and nano-clay on some properties of cementitious materials - A short guide for Civil Engineer[J]. Materials and Design, 2013, 52: 143-157.
14. Wu Y, Yi A, He J, et al. Mechanism of enhancement of mechanical properties of steam-cured UHPC by nano-C-S-H/PCE [J]. Bulletin of the Chinese Ceramic Society,2024,43(08):2797-2805.
15. Shi W, Gong Z, Liu K, et al. CO_2 corrosion behavior and microstructure of calcium aluminate cement-slag system [J]. Bulletin of the Chinese Ceramic Society,2023,42(10): 3695-3702.